Research Square

Preprints are preliminary reports that have not undergone peer review.
They should not be considered conclusive, used to inform clinical practice,
or referenced by the media as validated information.

S1P–S1PR1 Dysregulation Is Associated With Brain-Wide S1PR1 Molecular Covariance Reorganization and Compulsive-Like Behaviors in Sapap3-Deficient Mice

Ji-Hui Yue

yuejh@mail.sysu.edu.cn

the Fifth Affiliated Hospital of Sun Yat-Sen University

Yuchong Luo
Jianrong Ye
Sixuan Li
Shichuan Shen
Moyan Li
Yifan Qiu
Haolin Luo
Weijie Wang
Sirui Wu
Xiao Chen
Chunren Wei
Jiaying Huang
Weitian Xie
Linxin Man
Hongjun Jin
Shenglin Wen

Article

Keywords: Obsessive-compulsive disorder, Sapap3, Sphingosine-1-phosphate, S1PR1, PET imaging, Molecular covariance network, Individualized profiling

Posted Date: November 5th, 2026

DOI: https://doi.org/10.21203/rs.3.rs-11140159/v1

License: This work is licensed under a Creative Commons Attribution 4.0 International License.
Read Full License

Additional Declarations: The authors have declared there is **NO** conflict of interest to disclose

S1P–S1PR1 Dysregulation Is Associated With Brain-Wide S1PR1 Molecular Covariance Reorganization and Compulsive-Like Behaviors in Sapap3-Deficient Mice

Yuchong Luo1[+], Jianrong Ye1[+], Sixuan Li1[+], Shichuan Shen1, Moyan Li1, Yifan Qiu4, Haolin Luo2, Weijie wang1, Sirui Wu4, Xiao Chen1, Chunren Wei1, Jiaying Huang3, Weitian Xie3, Linxin Man3, Hongjun Jin4*, Shenglin Wen1* and Jihui Yue1*

1 Department of Psychiatry, the Fifth Affiliated Hospital, Sun Yat-Sen University, Zhuhai, Guangdong Province, 519000, China

2 Department of Critical Care Medicine, the Third Affiliated Hospital, Sun Yat-sen University, Guangzhou, Guangdong Province, 510630, China

3 School of Medicine, Sun Yat-sen University, Shenzhen, Guangdong Province, 518107, China

4 Guangdong Provincial Engineering Research Center of Molecular Imaging, the Fifth Affiliated Hospital, Sun Yat-sen University, Zhuhai, Guangdong Province, 519000, China

[+] These authors contributed equally to this work.

* Corresponding author:

Hongjun Jin, PhD, Guangdong Provincial Engineering Research Center of Molecular Imaging, the Fifth Affiliated Hospital, Sun Yat-sen University, Zhuhai, Guangdong Province, 519000, China, Email: jinhj3@mail.sysu.edu.cn

or

Shenglin Wen, Professor/Chief Physician, Department of Psychiatry, the Fifth Affiliated Hospital, Sun Yat-Sen University, Zhuhai, Guangdong Province, 519000, China, Email: wenshl@mail.sysu.edu.cn

or

Jihui Yue, MD, Department of Psychiatry, the Fifth Affiliated Hospital, Sun Yat-Sen University, Zhuhai, Guangdong Province, 519000, China, Email: yuejh@mail.sysu.edu.cn

ABSTRACT

Background: Obsessive-compulsive disorder (OCD) is a debilitating neuropsychiatric disorder with heterogeneous clinical manifestations and incompletely understood biological mechanisms. Although dysfunction of cortico-striato-thalamo-cortical (CSTC) circuits has been extensively implicated in OCD pathophysiology, emerging evidence indicates that compulsive symptoms also involve distributed alterations across large-scale brain systems, the molecular basis of which remains poorly understood. The sphingosine-1-phosphate (S1P)/S1P receptor 1 (S1PR1) axis regulates neuroimmune signaling, synaptic plasticity, and cellular homeostasis; however, its role in organizing brain-wide molecular architecture in compulsive pathology remains unknown.

Methods: Using *Sapap3* knockout (KO) mice, we integrated striatal metabolomics, S1PR1-targeted [^{18}F]TZ4877 PET imaging, ex vivo validation, whole-brain molecular covariance analysis, and individualized S1PR1 profile deviation scoring (PDS) to define multiscale alterations in S1P–S1PR1 biology. We further examined relationships among regional S1PR1 availability, molecular covariance architecture, individualized molecular deviation, and compulsive-like behaviors.

Results: *Sapap3* deficiency was associated with altered sphingolipid metabolism, characterized by increased S1P abundance in peripheral and central tissues and reduced regional S1PR1 availability across the brain. Whole-brain S1PR1 molecular covariance analysis revealed genotype-associated remodeling of receptor-level molecular organization, characterized by increased interregional covariance, reduced modular segregation, and hypothalamus-centered covariance alterations extending beyond classical CSTC regions. Individualized PDS analysis demonstrated that greater deviation from the normative S1PR1 spatial profile was associated with greater expression of compulsive-like phenotypes, including repetitive grooming and tic-like behaviors.

Conclusions: This study identifies S1P–S1PR1 dysregulation as a receptor-level molecular feature associated with large-scale brain organization in compulsive pathology. By integrating receptor-specific molecular

imaging, molecular covariance analysis, and individualized deviation profiling, we provide a systems-level framework linking distributed molecular organization with behavioral variability.

Keywords: Obsessive-compulsive disorder; *Sapap3*; Sphingosine-1-phosphate; S1PR1; PET imaging; Molecular covariance network; Individualized profiling

INTRODUCTION

Obsessive-compulsive disorder (OCD) is a chronic and disabling neuropsychiatric disorder affecting approximately 2–3% of the population and characterized by intrusive thoughts and repetitive behaviors that substantially impair daily functioning[1, 2]. Despite substantial advances in clinical and neurobiological research, the biological mechanisms underlying OCD re

main incompletely understood[3]. Although serotonin reuptake inhibitors remain first-line pharmacological treatments, a substantial proportion of patients show inadequate response or residual symptoms, highlighting the need to identify additional biological mechanisms underlying disease heterogeneity and treatment variability[4, 5].

Historically, OCD neurobiology has been largely conceptualized within the framework of cortico-striato-thalamo-cortical (CSTC) circuit dysfunction, particularly involving the orbitofrontal cortex, anterior cingulate cortex, and striatum[6]. Converging evidence from neuroimaging studies, lesion investigations, and animal models indicates that these circuits contribute to habit formation, behavioral inhibition, and cognitive control[7, 8]. However, CSTC-based models alone do not fully explain the clinical heterogeneity of OCD or the involvement of distributed brain systems beyond canonical circuitry, suggesting that molecular mechanisms underlying distributed brain dysfunction remain insufficiently characterized[1, 9].

Recent advances in network neuroscience have shifted the conceptual framework of psychiatric disorders from isolated regional dysfunction toward distributed alterations in large-scale brain organization[10, 11]. In OCD, neuroimaging studies have demonstrated abnormalities extending beyond classical CSTC regions, involving multiple systems including the amygdala, hippocampus, cerebellum, brainstem, and hypothalamus[7, 12]. Graph theoretical studies further demonstrate disrupted integration-segregation balance and abnormal modular organization across psychiatric disorders[11, 12]. These findings indicate that OCD may involve impaired organization of distributed neural systems in addition to abnormalities within specific circuit[13]. However, the

molecular substrates supporting large-scale brain organization remain poorly understood, partly because receptor-specific approaches capable of mapping molecular architecture across the whole brain are limited[14].

Sphingosine-1-phosphate (S1P) is a bioactive sphingolipid mediator that regulates neuroimmune signaling, synaptic plasticity, and cellular homeostasis[15]. Its effects are primarily mediated by S1P receptors, among which S1PR1 is widely expressed in the central nervous system and regulates neuronal adaptation, glial function, and neuroimmune communication[16, 17]. Emerging evidence suggests that sphingolipid signaling participates in neuroinflammatory regulation, synaptic remodeling, and stress-related processes relevant to psychiatric disorders[18]. Beyond its cellular functions, S1PR1 signaling has been implicated in neurovascular regulation and in mediating interactions between peripheral immune processes and central nervous system function[19]. These properties position S1PR1 as a potential molecular interface linking cellular state alterations with distributed brain organization. However, whether S1P–S1PR1 dysregulation contributes to compulsive pathology and brain-wide molecular organization remains unknown.

The *Sapap3* knockout (KO) mouse is a well-established model of compulsive-like behaviors, characterized by excessive repetitive grooming, anxiety-related phenotypes, and corticostriatal synaptic abnormalities[8]. Although this model has advanced understanding of CSTC mechanisms, most studies have focused on regional abnormalities within striatal circuits[8], leaving distributed molecular consequences insufficiently characterized. Moreover, conventional molecular imaging approaches generally rely on group-level comparisons and may not capture individual variability in molecular organization[20]. Recent individualized molecular deviation approaches provide a strategy for quantifying departures from normative molecular patterns; however, whether such approaches can reveal receptor-level molecular abnormalities associated with compulsive-like behaviors remains unknown[20, 21].

Here, we integrated untargeted metabolomics, S1PR1 receptor-specific [^{18}F]TZ4877 PET imaging, ex vivo autoradiography, immunofluorescence validation, whole-brain molecular covariance network analysis, and individualized S1PR1 profile deviation scoring to investigate whether S1P–S1PR1 alterations are associated

with brain-wide molecular organization in *Sapap3*-associated compulsive pathology. We hypothesized that S1P–S1PR1 axis alterations would be accompanied by widespread changes in receptor-level molecular organization and that individualized molecular deviation would capture variability associated with compulsive-like behaviors. This multiscale framework was designed to characterize the relationship between molecular alterations, whole-brain organization, and behavioral heterogeneity.

METHODS AND MATERIALS

I. Animals and Experimental Design

Male *Sapap3* KO mice and wild-type (WT) littermate controls were generated by breeding heterozygous *Sapap3*$^{+/-}$ mice. Because compulsive grooming phenotypes in KO mice progressively develop and stabilize in adulthood, 9-month-old mice were selected for behavioral and imaging studies[22, 23].

Animals were maintained under standard housing conditions, and all procedures were approved by the Institutional Animal Care and Use Committee (IACUC). Mice were randomly assigned to independent cohorts for behavioral, metabolomic, PET, and histological analyses. Investigators were blinded to genotype during behavioral testing, imaging analysis, and data processing. The brief experimental procedure is presented in Figure 1A and the detailed cohort allocation is provided in Supplementary Figure S1 and Table S1.

II. Behavioral Assessment

Behavioral assessments were performed during the dark phase, and recordings were analyzed by investigators blinded to genotype.

Compulsive-like repetitive behaviors were evaluated using spontaneous grooming assays with video-based behavioral scoring. Grooming videos were analyzed to quantify grooming frequency and duration, as well as repetitive tic-like events, digging behavior, and rearing activity[23-25]. Anxiety-related and exploratory behaviors were assessed using the open field test (OFT)[26] and elevated plus maze (EPM)[27]. Detailed behavioral

procedures and scoring criteria are described in Supplementary Methods.

III. Metabolomic Profiling and S1P Quantification

Untargeted metabolomic profiling was performed on striatal tissue using liquid chromatography–mass spectrometry (LC-MS/MS).

Differential metabolites were identified using multivariate and univariate statistical analyses. Alterations in sphingolipid-related metabolites were further validated by measuring S1P concentrations in serum and brain tissues using enzyme-linked immunosorbent assay (ELISA).

IV. S1PR1 PET Imaging and V_T Quantification

Whole-brain S1PR1 availability was assessed using receptor-targeted [^{18}F]TZ4877 PET imaging[28]. Dynamic microPET/CT scans were acquired following intravenous tracer administration. PET images were coregistered with MRI anatomical references, and regional tracer distribution was quantified using predefined brain regions based on the Ma–Benveniste–Mirrione mouse brain atlas.

Regional S1PR1 availability was quantified as total distribution volume (V_T) using kinetic modeling approaches described in Supplementary Methods[29].

V. Ex Vivo Autoradiography

Ex vivo autoradiography was performed to validate PET-derived regional [^{18}F]TZ4877 binding patterns.

VI. Whole-Brain S1PR1 Molecular Covariance Network and Individualized Profile Analysiss

Regional V_T values from 14 predefined brain regions were used to construct S1PR1 molecular covariance networks using established covariance network approaches[30, 31]. Pairwise Pearson correlations of regional V_T values were calculated to generate S1PR1 covariance matrices representing interregional molecular covariance patterns.

Binary and weighted covariance networks were constructed to evaluate global and regional network

properties, including network density, modularity, covariance strength, and node-level alterations[31]. A predefined correlation threshold was applied to generate high-confidence binary covariance networks, and sensitivity analyses across multiple thresholds were performed to evaluate the robustness of network topology.

Weighted network analysis was used to identify brain regions showing prominent alterations in molecular covariance organization. Because the hypothalamus demonstrated the largest change in node strength, hypothalamus-centered covariance patterns were subsequently examined[32].

To quantify individual variability in whole-brain S1PR1 molecular organization, an individualized S1PR1 profile deviation score (PDS) was calculated based on deviation from the WT reference profile[20, 21]. Higher PDS values indicate greater divergence from normative S1PR1 spatial organization. Detailed procedures for covariance network construction, threshold selection, permutation testing, and PDS calculation are described in Supplementary Methods.

VII. Statistical Analysis

Statistical analyses were performed using GraphPad Prism and R software. Group comparisons were performed using appropriate parametric or nonparametric tests. Correlations between molecular measures and behavioral phenotypes were assessed using Spearman correlation analysis, with multiple comparisons controlled using the Benjamini–Hochberg procedure. Network differences were evaluated using permutation-based statistics. All statistical tests were two-tailed, and $p < 0.05$ was considered statistically significant.

RESULTS

I. *Sapap3* KO Mice Display Robust Compulsive-Like Behavioral Abnormalities

Compared with WT littermates, *Sapap3* KO mice developed pronounced periorbital skin lesions resulting from excessive grooming, with severe cases exhibiting ocular injury (Figure 1B). Quantitative behavioral analysis confirmed significantly increased grooming bout frequency, grooming duration, and spontaneous tic-

like behaviors in *Sapap3* KO mice (Figure 1C–D; Table S2). In contrast, exploratory behaviors, including digging and rearing, were significantly reduced (Figure 1E–F; Table S2).

Consistent with previous reports, *Sapap3* KO mice also exhibited anxiety-like phenotypes, including reduced center exploration in the open field test and reduced open-arm exploration in the elevated plus maze (Figure S3; Table S2). Together, these findings confirm that *Sapap3* KO mice exhibit robust compulsive-like and anxiety-related behavioral phenotypes suitable for subsequent molecular analyses.

II. Striatal Metabolomic Profiling Reveals Altered Sphingolipid Metabolism and Increased S1P Abundance in *Sapap3* KO Mice

Given the central role of the striatum in CSTC circuitry and the enrichment of *Sapap3* expression in this region, we performed untargeted metabolomic profiling to determine whether compulsive-like pathology was accompanied by metabolic alterations relevant to S1P signaling.

Principal component analysis demonstrated clear metabolic separation between *Sapap3* KO and WT mice (Figure 1G), indicating widespread metabolic remodeling in the striatum. Among 2,645 detected metabolites, 119 satisfied the predefined criteria for differential abundance (adjusted $q < 0.05$ and $|\log_2 FC| > 1$), including 52 increased and 67 decreased metabolites (Figure 1H). Lipid-related metabolites represented the largest altered metabolic category (46.22%; Figure S4).

Among the altered metabolites, S1P emerged as a prominent dysregulated sphingolipid metabolite. Multiple metabolites involved in S1P biosynthesis, including sphingosine, sphingosine phosphate, and dihydrosphingosine, were also increased (Figure 1I). KEGG pathway enrichment and GSEA consistently identified sphingolipid metabolism and sphingolipid signaling as significantly altered pathway (Figure 1J-K).

ELISA independently confirmed elevated S1P concentrations in serum, striatum, and prefrontal cortex (Figure 1L; Table S3), indicating that altered sphingolipid metabolism extends beyond the striatum and involves both central and peripheral compartments. Given that S1P exerts its biological effects primarily

through S1PR1, we next examined whether altered sphingolipid metabolism was accompanied by changes in brain-wide S1PR1 availability.

III. S1PR1-Targeted PET Imaging Reveals Brain-Wide Reductions in S1PR1 Availability

To determine whether elevated S1P abundance was associated with alterations in receptor availability, we quantified whole-brain S1PR1 availability using [^{18}F]TZ4877 PET imaging.

Quantitative PET analysis demonstrated significantly reduced S1PR1 V_T values across widespread cortical and subcortical regions in *Sapap3* KO mice (Figure 2A, B; Figure S5; Table S4). Reductions were observed in both canonical CSTC structures and multiple extra-CSTC regions, indicating that altered S1PR1 availability extended beyond corticostriatal circuitry. Ex vivo autoradiography independently confirmed reduced regional [^{18}F]TZ4877 binding in representative brain regions (Figure 2C, D; Figure S6; Table S5). The concordance between in vivo PET imaging and ex vivo autoradiography supports the robustness of the observed reductions in S1PR1 availability across the brain. To determine whether these imaging findings reflected receptor-level alterations at the tissue level, we next examined regional S1PR1 expression by immunofluorescence.

IV. Immunofluorescence Validation Confirms Reduced S1PR1 Immunoreactivity in *Sapap3* KO Mice

To determine whether reduced PET-derived S1PR1 availability was accompanied by tissue-level changes in receptor immunoreactivity, we performed immunofluorescence analysis in the cortex and striatum, two regions critically involved in CSTC circuitry.

Quantitative analysis demonstrated significant reductions in S1PR1 puncta density, puncta area, and integrated fluorescence intensity in both the cortex and striatum (Figure 3A–D; Table S6). Together with PET imaging and ex vivo autoradiography, these findings provide convergent evidence that reduced S1PR1 availability in *Sapap3* KO mice is accompanied by decreased regional S1PR1 immunoreactivity. Given the widespread distribution of these receptor-level alterations, we next investigated whether they were associated with reorganization of whole-brain S1PR1 molecular covariance networks.

V. Reduced S1PR1 Availability Is Associated With Compulsive-like Behaviors

To determine whether regional S1PR1 availability was associated with behavioral phenotypes, we performed Spearman correlation analyses between regional PET-derived V_T values and behavioral measurements, followed by false discovery rate (FDR) correction.

Grooming bout frequency and grooming duration exhibited widespread negative associations with regional S1PR1 availability. Similarly, tic-like behavior frequency showed significant negative associations across overlapping cortical and subcortical regions (Figure 3E). In contrast, digging behavior showed positive associations with regional S1PR1 availability, whereas rearing behavior was not significantly associated with regional V_T values following FDR correction (Figure 3E).

Anxiety-related behavioral measures, including center exploration in the open field test and open-arm exploration in the elevated plus maze, exhibited distinct regional association patterns compared with compulsive-like behaviors (Figure S7). Together, these findings suggest that regional S1PR1 availability is preferentially associated with compulsive-like behavioral phenotypes rather than generalized behavioral dysfunction. Because these behavioral associations were distributed across multiple brain regions rather than confined to individual structures, we next investigated whether S1PR1 alterations were accompanied by reorganization of whole-brain molecular covariance networks.

VI. *Sapap3* Deficiency Is Associated With Brain-wide Reorganization Of S1PR1 Molecular Covariance Networks

To determine whether distributed S1PR1 alterations were accompanied by changes in large-scale molecular organization, we constructed whole-brain S1PR1 molecular covariance networks based on interregional correlations of PET-derived V_T values across 14 predefined brain regions (Figure 4A–C).

Pairwise covariance analysis revealed a marked shift toward higher regional S1PR1 covariance in *Sapap3* KO mice compared with WT controls, indicating altered organization of receptor availability across the brain.

The median Pearson correlation coefficient increased from 0.81 in WT mice to 0.95 in KO mice (Figure S8A).

Using a predefined high-confidence covariance threshold ($|r| > 0.85$), KO mice exhibited substantially increased network density compared with WT mice, with 86 retained covariance relationships (density = 0.945) versus 36 relationships (density = 0.396), respectively (Figure 4D–E). Permutation testing confirmed that the observed increase in network density exceeded random expectations (Δdensity = 0.549, $p = 0.023$, Figure S8).

Edge-level analysis demonstrated extensive remodeling of S1PR1 molecular covariance architecture. KO mice exhibited 51 genotype-specific covariance relationships, whereas only one WT-specific relationship was identified, indicating widespread emergence of altered interregional molecular covariance patterns.

Louvain community detection further revealed disruption of modular organization. WT mice displayed two distinct molecular covariance modules (modularity Q = 0.287), whereas KO networks collapsed into a single integrated module encompassing all 14 brain regions (Q = 0; Figure 4F–G).

Together, these findings indicate that Sapap3 deficiency is associated with a shift from modular segregation toward increased integration of brain-wide S1PR1 molecular covariance organization. To identify the regional contributors underlying this network-level reorganization, we next examined node-level alterations and hypothalamus-centered covariance patterns.

VII. Weighted Network Analysis Identifies the Hypothalamus as a Key Node in S1PR1 Network Reorganization

To identify brain regions contributing most strongly to S1PR1 network alterations, we performed weighted network analysis using regional V_T correlations and calculated changes in node strength ($\Delta S = S_{KO} - S_{WT}$, Figure 5A, B).

The hypothalamus exhibited the largest increase in node strength ($\Delta S = 3.97$), followed by the brainstem ($\Delta S = 3.84$) and superior colliculus ($\Delta S = 3.16$). In contrast, the striatum, a canonical region implicated in OCD models, showed relatively limited changes in network strength ($\Delta S = 1.15$; ranked 14th among all

regions). The increase in hypothalamic network strength was approximately 3.46-fold greater than that observed in the striatum (Figure 5B).

Permutation testing confirmed a significant increase in hypothalamic node strength ($p = 0.03$), indicating that *Sapap3* deficiency is associated with distributed network reorganization rather than changes restricted to classical CSTC regions.

Edge-level analysis further revealed selective strengthening of hypothalamic connections with sensorimotor-related regions, including the Inferior colliculus ($\Delta r = 0.606$), cortex ($\Delta r = 0.527$), and superior colliculus ($\Delta r = 0.446$), whereas connections with amygdala and brainstem showed minimal changes (Figure 5C). Notably, increased hypothalamic network centrality was not simply attributable to local S1PR1 reduction. The magnitude of hypothalamic connectivity changes did not consistently correspond to regional V_T decreases, suggesting that enhanced hypothalamic hubness primarily reflected network reorganization rather than isolated receptor loss (Figure 5D).

These findings suggest that the hypothalamus emerges as a key organizational hub within the remodeled S1PR1 network, potentially reflecting altered integration between homeostatic and sensorimotor systems.

VIII. Individualized S1PR1 Profile Deviation Quantifies Receptor-level Molecular Variability Associated With Compulsive-like Behaviors

Although group-level network analyses revealed widespread reorganization of S1PR1 organization, they do not capture individual variability in molecular alterations. Therefore, we developed an individualized S1PR1 PDS to quantify the extent to which each animal deviated from the WT reference S1PR1 spatial pattern (Figure 5E).

Compared with WT mice, KO mice exhibited significantly higher PDS values, indicating greater deviation from the WT-reference S1PR1 organization (Figure 5F). Regional deviation mapping revealed that molecular alterations were not uniformly distributed but were concentrated in specific regions, including the

periaqueductal gray, brainstem, cerebellum, basal forebrain, and striatum (Figure 5G).

Importantly, individual PDS values were positively associated with compulsive-like behaviors, including grooming frequency, grooming duration, and tic-like behaviors (Figure 5H-J). These findings indicate that individualized molecular deviation provides a quantitative measure of receptor-level spatial variability associated with behavioral severity.

IX. An Integrated Framework Linking S1P–S1PR1 Alterations With Molecular Network Organization and Behavioral Variability

To integrate the multi-level findings, we constructed a conceptual framework summarizing associations among S1P metabolism, S1PR1 availability, whole-brain molecular organization, and compulsive-like behaviors (Figure 6). *Sapap3* deficiency was associated with increased S1P abundance, reduced S1PR1 availability, brain-wide molecular covariance reorganization characterized by increased connectivity and reduced modular organization, and individualized S1PR1 deviations linked to behavioral severity. This framework highlights the association between S1P–S1PR1 alterations, distributed molecular network dysregulation, and compulsive-like phenotypes.

DISCUSSION

Obsessive-compulsive disorder is increasingly recognized as a disorder involving distributed brain systems rather than dysfunction confined to canonical CSTC circuits[7, 33]. However, the receptor-level molecular mechanisms underlying large-scale brain organization in compulsive pathology remain poorly understood. In the present study, we show that *Sapap3* deficiency is associated with coordinated alterations spanning sphingolipid metabolism, brain-wide S1PR1 availability, molecular covariance organization, and individualized molecular heterogeneity. By integrating metabolomics, receptor-specific PET imaging, whole-brain molecular covariance analysis, and individualized profile deviation scoring, we provide a multiscale

framework linking molecular alterations with distributed brain organization and behavioral variability. Rather than challenging the established CSTC model, our findings extend current circuit-based concepts by suggesting that compulsive-like pathology is accompanied by distributed alterations in receptor-level molecular architecture across the brain.

A major finding of this study is the identification of S1P–S1PR1 dysregulation as a receptor-level molecular alteration associated with compulsive-like pathology. S1P is a pleiotropic sphingolipid mediator that regulates neuroimmune communication, synaptic plasticity, vascular homeostasis, and cellular adaptation through activation of a family of G protein-coupled receptors[15, 34]. Among these receptors, S1PR1 is the predominant subtype in the central nervous system and has been implicated in neuronal survival, glial function, immune signaling, and maintenance of synaptic integrity[16, 35]. Although S1P signaling has been linked to several neurological and psychiatric disorders, previous studies have largely focused on regional or cellular alterations[36]. Our findings extend this literature by showing that S1P-related metabolic abnormalities are associated not only with reduced regional S1PR1 availability but also with alterations in receptor-level molecular organization across distributed brain systems.

Although the present study demonstrates a robust association between *Sapap3* deficiency and S1P–S1PR1 dysregulation, the mechanistic relationship between postsynaptic scaffolding abnormalities and sphingolipid remodeling remains unresolved. *Sapap3* is an essential component of the postsynaptic density that maintains excitatory synaptic organization within corticostriatal medium spiny neurons[8, 37]. Loss of Sapap3 disrupts glutamatergic transmission and produces well-characterized compulsive-like phenotypes[8]. Whether these synaptic abnormalities directly influence sphingolipid metabolism, however, remains unknown. One possibility is that altered neuronal activity and neuron–glia communication reshape local lipid metabolism, thereby contributing to broader changes in receptor availability[15, 38]. Alternatively, sphingolipid remodeling may represent a compensatory response to chronic synaptic dysfunction. Distinguishing these possibilities will require future studies integrating cell-type-specific molecular profiling, electrophysiology, and targeted

manipulation of S1P signaling pathways.

The coexistence of elevated S1P levels and reduced S1PR1 availability raises an important mechanistic question regarding the directionality of S1P–S1PR1 dysregulation. Reduced S1PR1 availability may reflect either a pathogenic alteration or an adaptive response to increased S1P. Elevated S1P could promote receptor desensitization, internalization, or adaptive downregulation under specific signaling conditions[39]. Conversely, reduced S1PR1 signaling may impair neuronal plasticity and neuroimmune regulation[35, 40]. The present data cannot distinguish among these possibilities or establish whether altered S1P concentrations precede changes in receptor availability. Future studies combining pharmacological or genetic manipulation of S1PR1 with assessment of downstream signaling pathways, including ERK and AKT signaling, will be required to clarify whether S1P–S1PR1 dysregulation represents a primary molecular vulnerability, a secondary consequence of circuit dysfunction, or a compensatory adaptation [41].

Beyond these central molecular alterations, the concordant elevation of S1P in serum and brain tissue raises a potentially important question regarding peripheral–central sphingolipid relationships. While circulating S1P is known to participate in systemic immune and vascular regulation[42, 43], the present data cannot determine whether increased serum S1P reflects peripheral metabolic activation, altered transport or exchange across the blood–brain barrier, altered central contribution to circulating S1P levels, or partially independent metabolic alterations occurring in both compartments. Nevertheless, the parallel elevation across central and peripheral compartments raises possibility that circulating S1P could reflect broader alterations in sphingolipid homeostasis associated with compulsive-like pathology. Future studies integrating isotope tracing, blood–brain barrier transport assessment, and compartment-specific manipulation of sphingolipid metabolism will be essential to establish the origin and directionality of these S1P alterations[44, 45].

The widespread reduction in S1PR1 availability observed by PET imaging provides an in vivo molecular perspective on compulsive pathology that extends beyond regional neurochemical measurements. Unlike conventional ex vivo approaches, receptor-specific PET imaging enables quantitative assessment of receptor

availability across distributed brain regions within an intact biological system[46, 47]. Importantly, the concordance between PET imaging, autoradiography, and immunofluorescence supports the robustness of the observed receptor-level alterations while emphasizing that PET-derived V_T reflects receptor availability rather than receptor signaling or functional activity. Consequently, the PET findings should be interpreted as evidence of altered S1PR1 availability and spatial distribution rather than direct evidence of altered downstream receptor signaling.

Beyond regional receptor alterations, the principal conceptual advance of this study lies in demonstrating brain-wide reorganization of S1PR1 molecular covariance architecture. Molecular covariance networks characterize coordinated regional variation in receptor availability across the brain and therefore provide information that is fundamentally different from anatomical projections or functional connectivity[32, 48]. Rather than quantifying physical connections between brain regions, this framework captures the spatial organization of receptor-level molecular states[30]. The increased interregional covariance and loss of modular segregation observed in *Sapap3*-deficient mice indicate a shift from a more differentiated modular organization toward a more globally integrated pattern of receptor-level molecular covariance[32, 49]. Although the biological mechanisms underlying this reorganization remain unknown, these findings suggest that compulsive-like pathology may involve alterations not only in the magnitude of regional molecular abnormalities but also in the systems-level organization of receptor availability across distributed brain systems.

These observations also broaden current circuit-based models of OCD. The CSTC framework has been instrumental in defining the neural circuitry underlying compulsive behaviors, particularly through abnormalities involving corticostriatal communication[6, 50]. Nevertheless, accumulating evidence indicates that OCD is associated with distributed abnormalities involving limbic, cerebellar, brainstem, and hypothalamic systems in addition to canonical CSTC regions[7, 33]. Our findings are consistent with this evolving perspective by demonstrating that receptor-level molecular alterations are organized across multiple brain systems rather than being restricted to corticostriatal nodes. Importantly, these findings should not be viewed as replacing the

CSTC model but rather as complementing it by introducing a molecular organizational dimension for characterizing how regional receptor abnormalities are coordinated across distributed brain systems.

An additional finding was the identification of the hypothalamus as a prominent node within the reorganized S1PR1 molecular covariance network. Although the hypothalamus has received comparatively less attention in OCD than classical CSTC regions, it plays central roles in neuroendocrine regulation, autonomic homeostasis, and integration of central and peripheral physiological signals[51, 52]. The prominent network position of the hypothalamus therefore raises the possibility that this region participates disproportionately in the altered pattern of S1PR1 molecular covariance observed in *Sapap3*-deficient mice. However, the present study does not establish a causal role for hypothalamic S1PR1 signaling, and future studies combining molecular imaging with region-specific manipulation and endocrine assessment will be necessary to determine its functional significance.

Beyond identifying group-level alterations in S1PR1 molecular organization, this study further addressed an important challenge in psychiatric neuroscience: biological heterogeneity among individuals with similar behavioral phenotypes. Conventional case–control comparisons are essential for identifying disease-associated alterations but may obscure meaningful variation in molecular organization across individuals[20]. By quantifying deviations from a WT-derived reference pattern, the individualized S1PR1 PDS provided an approach for characterizing subject-specific divergence in receptor-level molecular architecture. The association between higher PDS values and more severe compulsive-like behaviors suggests that the degree of molecular deviation may capture biologically relevant variability underlying behavioral expression. However, these findings should be interpreted as an association rather than a deterministic measure of symptom severity [53]. Future studies incorporating longitudinal PET assessments, larger cohorts, and cross-model validation will be required to determine the stability, reproducibility, and biological specificity of individualized S1PR1 profiles.

More broadly, combining receptor-specific molecular imaging with systems-level covariance analysis and

individualized deviation profiling provides a potential framework for investigating biological heterogeneity in psychiatric disorders. PET enables in vivo characterization of molecular targets while preserving regional information, whereas covariance analysis captures how receptor-level molecular states are organized across distributed brain systems[54, 55]. When integrated with individualized profiling, this approach may facilitate future studies aimed at identifying biologically meaningful subgroups and examining molecular variation in relation to clinical phenotypes or treatment response[20, 56]. However, the present findings should be regarded as a conceptual framework rather than evidence for an immediately applicable clinical biomarker, and validation in human cohorts will be essential before clinical translation can be considered.

Several limitations should be considered when interpreting the present findings. First, this study identifies associations between S1P–S1PR1 dysregulation, molecular covariance organization, and compulsive-like behaviors but does not establish causal relationships. Future studies employing pharmacological or genetic manipulation of S1PR1 signaling will be necessary to determine whether experimentally modifying S1PR1 signaling alters receptor availability, molecular covariance patterns, and behavioral phenotypes. Second, although the *Sapap3*-deficient mouse is a well-established model of compulsive-like behavior, it represents only one aspect of the biological heterogeneity observed in human OCD[3]. Validation across additional preclinical models and, ultimately, clinical PET studies will therefore be essential to determine the generalizability of the present findings. Third, PET-derived V_T reflects receptor availability rather than receptor activation or downstream signaling. Alterations in V_T may reflect multiple biological processes, including changes in receptor abundance, trafficking, internalization, or other factors affecting tracer binding and should not be interpreted as direct measures of S1PR1 functional activity [46]. Fourth, molecular covariance networks quantify coordinated interregional variation in receptor availability at the group level and should not be interpreted as direct measures of anatomical or functional connectivity. Instead, they represent a systems-level description of receptor organization across the brain. Finally, although serum and brain S1P concentrations were elevated in parallel, the present study cannot determine the origin, temporal sequence, or

directionality of these alterations. Future investigations incorporating isotope tracing, blood–brain barrier transport analyses, and compartment-specific manipulation of sphingolipid metabolism will be required to clarify the relationships between peripheral and central S1P homeostasis.

In summary, our findings identify S1P–S1PR1 dysregulation as a receptor-level molecular feature associated with compulsive-like pathology and show that these alterations extend from regional receptor availability to brain-wide molecular covariance organization and inter-individual molecular heterogeneity. These results complement current circuit-based models of OCD by introducing a systems-level molecular dimension to the biological architecture of compulsive pathology. Future studies will be required to determine the causal mechanisms underlying S1P–S1PR1 dysregulation and to establish whether similar patterns of receptor-level molecular organization are present in human OCD.

REFERENCES

1. Pauls DL, Abramovitch A, Rauch SL, Geller DA. Obsessive-compulsive disorder: an integrative genetic and neurobiological perspective. *Nat Rev Neurosci* 2014; **15**(6)**:** 410–424.

2. Ruscio AM, Stein DJ, Chiu WT, Kessler RC. The epidemiology of obsessive-compulsive disorder in the National Comorbidity Survey Replication. *Mol Psychiatry* 2010; **15**(1)**:** 53–63.

3. Stein DJ, Costa DLC, Lochner C, Miguel EC, Reddy YCJ, Shavitt RG *et al.* Obsessive-compulsive disorder. *Nat Rev Dis Primers* 2019; **5**(1)**:** 52.

4. Fineberg NA, Dell'Osso B, Albert U, Maina G, Geller D, Carmi L *et al.* Early intervention for obsessive compulsive disorder: An expert consensus statement. *Eur Neuropsychopharmacol* 2019; **29**(4)**:** 549–565.

5. Pittenger C, Bloch MH. Pharmacological treatment of obsessive-compulsive disorder. *Psychiatr Clin North Am* 2014; **37**(3)**:** 375–391.

6. Saxena S, Brody AL, Schwartz JM, Baxter LR. Neuroimaging and frontal-subcortical circuitry in obsessive-compulsive disorder. *Br J Psychiatry Suppl* 1998; (35)**:** 26–37.

7. Milad MR, Rauch SL. Obsessive-compulsive disorder: beyond segregated cortico-striatal pathways. *Trends Cogn Sci* 2012; **16**(1)**:** 43–51.

8. Welch JM, Lu J, Rodriguiz RM, Trotta NC, Peca J, Ding J-D *et al.* Cortico-striatal synaptic defects and OCD-like behaviours in Sapap3-mutant mice. *Nature* 2007; **448**(7156)**:** 894–900.

9. Beucke JC, Sepulcre J, Talukdar T, Linnman C, Zschenderlein K, Endrass T *et al.* Abnormally high degree connectivity of the orbitofrontal cortex in obsessive-compulsive disorder. *JAMA Psychiatry* 2013; **70**(6)**:** 619–629.

10. Bullmore E, Sporns O. The economy of brain network organization. *Nat Rev Neurosci* 2012; **13**(5)**:** 336–349.

11. Menon V. Large-scale brain networks and psychopathology: a unifying triple network model. *Trends Cogn Sci* 2011; **15**(10)**:** 483–506.

12. Rubinov M, Sporns O. Complex network measures of brain connectivity: uses and interpretations. *Neuroimage* 2010; **52**(3)**:** 1059–1069.

13. Bassett DS, Sporns O. Network neuroscience. *Nat Neurosci* 2017; **20**(3)**:** 353–364.

14. Mintun MA, Raichle ME, Kilbourn MR, Wooten GF, Welch MJ. A quantitative model for the in vivo assessment of drug binding sites with positron emission tomography. *Ann Neurol* 1984; **15**(3)**:** 217–227.

15. Maceyka M, Spiegel S. Sphingolipid metabolites in inflammatory disease. *Nature* 2014; **510**(7503)**:** 58–67.

16. Chun J, Hla T, Lynch KR, Spiegel S, Moolenaar WH. International Union of Basic and Clinical

Pharmacology. LXXVIII. Lysophospholipid receptor nomenclature. *Pharmacol Rev* 2010; **62**(4)**:** 579–587.

17. Healy LM, Antel JP. Sphingosine-1-Phosphate Receptors in the Central Nervous and Immune Systems. *Curr Drug Targets* 2016; **17**(16)**:** 1841–1850.

18. van Kruining D, Luo Q, van Echten-Deckert G, Mielke MM, Bowman A, Ellis S *et al.* Sphingolipids as prognostic biomarkers of neurodegeneration, neuroinflammation, and psychiatric diseases and their emerging role in lipidomic investigation methods. *Adv Drug Deliv Rev* 2020; **159:** 232–244.

19. Mao-Draayer Y, Sarazin J, Fox D, Schiopu E. The sphingosine-1-phosphate receptor: A novel therapeutic target for multiple sclerosis and other autoimmune diseases. *Clin Immunol* 2017; **175:** 10–15.

20. Marquand AF, Kia SM, Zabihi M, Wolfers T, Buitelaar JK, Beckmann CF. Conceptualizing mental disorders as deviations from normative functioning. *Mol Psychiatry* 2019; **24**(10)**:** 1415–1424.

21. Rutherford S, Kia SM, Wolfers T, Fraza C, Zabihi M, Dinga R *et al.* The normative modeling framework for computational psychiatry. *Nat Protoc* 2022; **17**(7)**:** 1711–1734.

22. Burguière E, Monteiro P, Feng G, Graybiel AM. Optogenetic stimulation of lateral orbitofronto-striatal pathway suppresses compulsive behaviors. *Science* 2013; **340**(6137)**:** 1243–1246.

23. Lamothe H, Schreiweis C, Mondragón-González LS, Rebbah S, Lavielle O, Mallet L *et al.* The Sapap3(-/-) mouse reconsidered as a comorbid model expressing a spectrum of pathological repetitive behaviours. *Transl Psychiatry* 2023; **13**(1)**:** 26.

24. Partridge KJ, Hillhouse TM. Differential effects of repeated fluoxetine and ketamine administration on behavioral and pharmacological stressor-induced depression of digging behavior in mice. *Exp Clin Psychopharmacol* 2024; **32**(5)**:** 506–517.

25. Sturman O, Germain PL, Bohacek J. Exploratory rearing: a context- and stress-sensitive behavior recorded in the open-field test. *Stress* 2018; **21**(5)**:** 443–452.

26. Prut L, Belzung C. The open field as a paradigm to measure the effects of drugs on anxiety-like behaviors: a review. *Eur J Pharmacol* 2003; **463**(1-3)**:** 3–33.

27. Walf AA, Frye CA. The use of the elevated plus maze as an assay of anxiety-related behavior in rodents. *Nat Protoc* 2007; **2**(2)**:** 322–328.

28. Wang L, Bi L, Qiu Y, Huang G, Ye P, Liu Y *et al.* Effectiveness of electro-acupuncture for cognitive improvement on Alzheimer's disease quantified via PET imaging of sphingosine-1-phosphate receptor 1. *Alzheimers Dement* 2024; **20**(12)**:** 8331–8345.

29. Logan J, Fowler JS, Volkow ND, Wang GJ, Ding YS, Alexoff DL. Distribution volume ratios without blood sampling from graphical analysis of PET data. *J Cereb Blood Flow Metab* 1996; **16**(5)**:** 834–840.

30. Alexander-Bloch A, Giedd JN, Bullmore E. Imaging structural co-variance between human brain regions. *Nat Rev Neurosci* 2013; **14**(5)**:** 322–336.

31. Crossley NA, Mechelli A, Scott J, Carletti F, Fox PT, McGuire P *et al.* The hubs of the human connectome are generally implicated in the anatomy of brain disorders. *Brain* 2014; **137**(Pt 8)**:** 2382–2395.

32. Bullmore E, Sporns O. Complex brain networks: graph theoretical analysis of structural and functional systems. *Nat Rev Neurosci* 2009; **10**(3)**:** 186–198.

33. Piras F, Piras F, Caltagirone C, Spalletta G. Brain circuitries of obsessive compulsive disorder: a systematic review and meta-analysis of diffusion tensor imaging studies. *Neurosci Biobehav Rev* 2013; **37**(10 Pt 2)**:** 2856–2877.

34. van Echten-Deckert G. The role of sphingosine 1-phosphate metabolism in brain health and disease. *Pharmacol Ther* 2023; **244:** 108381.

35. Choi JW, Gardell SE, Herr DR, Rivera R, Lee CW, Noguchi K *et al.* FTY720 (fingolimod) efficacy in an animal model of multiple sclerosis requires astrocyte sphingosine 1-phosphate receptor 1 (S1P1) modulation. *Proc Natl Acad Sci U S A* 2011; **108**(2)**:** 751–756.

36. Hait NC, Maiti A. The Role of Sphingosine-1-Phosphate and Ceramide-1-Phosphate in Inflammation and Cancer. *Mediators Inflamm* 2017; **2017:** 4806541.

37. Kim E, Sheng M. PDZ domain proteins of synapses. *Nat Rev Neurosci* 2004; **5**(10)**:** 771–781.

38. Burg N, Salmon JE, Hla T. Sphingosine 1-phosphate receptor-targeted therapeutics in rheumatic diseases. *Nat Rev Rheumatol* 2022; **18**(6)**:** 335–351.

39. Rosen H, Stevens RC, Hanson M, Roberts E, Oldstone MB. Sphingosine-1-phosphate and its receptors: structure, signaling, and influence. *Annu Rev Biochem* 2013; **82:** 637–662.

40. Yanagida K, Liu CH, Faraco G, Galvani S, Smith HK, Burg N *et al.* Size-selective opening of the blood-brain barrier by targeting endothelial sphingosine 1-phosphate receptor 1. *Proc Natl Acad Sci U S A* 2017; **114**(17)**:** 4531–4536.

41. Spiegel S, Milstien S. The outs and the ins of sphingosine-1-phosphate in immunity. *Nat Rev Immunol* 2011; **11**(6)**:** 403–415.

42. Proia RL, Hla T. Emerging biology of sphingosine-1-phosphate: its role in pathogenesis and therapy. *J Clin Invest* 2015; **125**(4)**:** 1379–1387.

43. Cartier A, Hla T. Sphingosine 1-phosphate: Lipid signaling in pathology and therapy. *Science* 2019; **366**(6463).

44. Maceyka M, Sankala H, Hait NC, Le Stunff H, Liu H, Toman R *et al.* SphK1 and SphK2, sphingosine kinase isoenzymes with opposing functions in sphingolipid metabolism. *J Biol Chem* 2005; **280**(44)**:** 37118–37129.

45. Daneman R, Prat A. The blood-brain barrier. *Cold Spring Harb Perspect Biol* 2015; **7**(1)**:** a020412.

46. Laruelle M. Imaging synaptic neurotransmission with in vivo binding competition techniques: a critical review. *J Cereb Blood Flow Metab* 2000; **20**(3)**:** 423–451.

47. Bronte A, Prieto E, Quincoces G, Erro E, Arbizu J. The basics of PET molecular imaging in neurodegenerative disorders with dementia and/or parkinsonism. *Eur Radiol* 2025; **35**(8)**:** 4621–4634.

48. Horwitz B, Duara R, Rapoport SI. Intercorrelations of glucose metabolic rates between brain regions: application to healthy males in a state of reduced sensory input. *J Cereb Blood Flow Metab* 1984; **4**(4)**:** 484–499.

49. Newman ME. Modularity and community structure in networks. *Proc Natl Acad Sci U S A* 2006; **103**(23)**:** 8577–8582.

50. Graybiel AM, Rauch SL. Toward a neurobiology of obsessive-compulsive disorder. *Neuron* 2000; **28**(2)**:** 343–347.

51. Herman JP, McKlveen JM, Ghosal S, Kopp B, Wulsin A, Makinson R *et al.* Regulation of the Hypothalamic-Pituitary-Adrenocortical Stress Response. *Compr Physiol* 2016; **6**(2)**:** 603–621.

52. Ulrich-Lai YM, Herman JP. Neural regulation of endocrine and autonomic stress responses. *Nat Rev Neurosci* 2009; **10**(6)**:** 397–409.

53. Insel TR, Cuthbert BN. Medicine. Brain disorders? Precisely. *Science* 2015; **348**(6234)**:** 499–500.

54. Ferrando R, Hernandes D, Ghini BG, Coutinho AM. PET Imaging in Psychiatric Disorders. *Semin Nucl Med* 2025; **55**(4)**:** 587–604.

55. Reed MB, Cocchi L, Sander CY, Chen J, Matheson GJ, Fisher P *et al.* Connecting the dots: approaching a standardized nomenclature for molecular connectivity in positron emission tomography. *Eur J Nucl Med Mol Imaging* 2025; **53**(1)**:** 48–58.

56. Maccioni L, Giacomel A, Pinamonti M, De Francisci M, Del Pup F, Giubergia A *et al.* Quantitative neuroimaging meets normative modelling: the last mile for precision medicine applications. *Neuroimage* 2026; **325:** 121637.

AUTHOR CONTRIBUTIONS

Y.L., J.Y., S.W., and H.J. designed, performed, and analyzed the experiments. S.L., S.S., Y.Q., and S.W. participated in radiochemistry and HPLC quality control. Y.L., M.L., and H.L. carried out the PET analysis. W.W. and C.W. conducted the metabolomics analysis. X.C., J.H., L.M., and W.X. participated in immunofluorescence staining. Y.L., J.Y., S.L., S.S., M.L., and H.L. contributed to the experimental design suggestions and manuscript revision. S.W. and H.J. wrote the manuscript. J.Y. supervised the project and directed the experiments.

During the preparation of this manuscript, the authors used OpenAI's ChatGPT to assist with language refinement and improvement of manuscript clarity. The use of this tool was limited to editorial assistance, including polishing scientific writing and improving readability. ChatGPT was not used for data analysis, interpretation of results, generation of scientific conclusions, or decision-making regarding the research. The authors have reviewed and revised all AI-assisted content and take full responsibility for the accuracy, integrity, and originality of the manuscript.

The authors report no biomedical financial interests or potential conflicts of interest.

FUNDING SOURCES

This work was supported by the National Natural Science Foundation of China (82372004, 81871382, 82150610508), the Science and Technology Development Fund, Macau SAR (FDCT, 0007/2022/AKP), the Key Realm R&D Program of Guangdong Province (2018B030337001), and the Natural Science Foundation of Guangdong Province (2019A1515011308).

ARTICLE INFORMATION

From the Department of Psychiatry of the Fifth Affiliated Hospital of Sun Yat-sen University (Y.L., J.Y., S.L., S.S., M.L., W.W., X.C., C.W., S.W., J.Y.), Sun Yat-sen University, Guangdong Province, China; Guangdong Provincial Engineering Research Center of Molecular Imaging (Y.Q., S.W., H.J.), Sun Yat-sen University, Guangdong Province, China; The Department of Critical Care Medicine of the Third Affiliated Hospital of Sun Yat-sen University (H.L.), Sun Yat-sen University, Guangdong Province, China; School of

Medicine (J.H., L.M., W.X.), Sun Yat-sen University, Guangdong Province, China.

Y.L., J.Y., and S.L. contributed equally to this work.

Address correspondence to Jihui Yue, at yuejh@mail.sysu.edu.cn

ETHICS APPROVAL

All methods were performed in accordance with the relevant guidelines and regulations. All experiments were approved by the institutional Animal Care and Use Committee of the Animal Facility of the Fifth Affiliated Hospital of Sun Yat-sen University (00574).

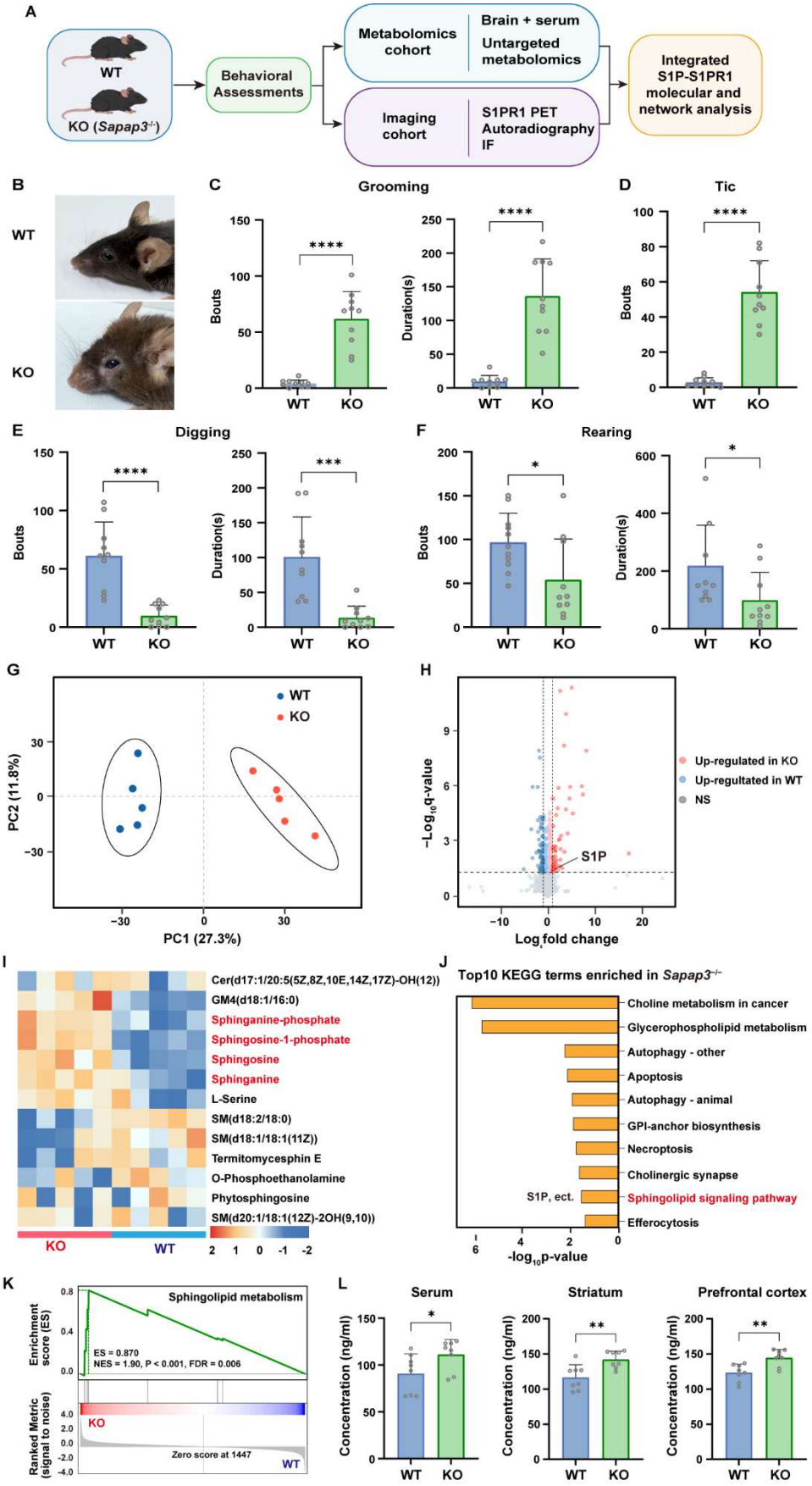


Figure 1. Behavioral characterization and identification of sphingolipid metabolic alterations in *Sapap3*-deficient mice.

(A) Schematic overview of the experimental workflow. (B) Representative images of periorbital skin lesions in *Sapap3* KO mice. (C) Quantification of grooming bout frequency and grooming duration. (D) Quantification of tic-like behaviors frequency. (E) Quantification of digging behavior. (F) Quantification of rearing behavior. (G) PCA of striatal metabolomic profiles from WT and *Sapap3* KO mice. (H) Volcano plot showing differentially altered metabolites between genotypes. (I) Heatmap showing sphingolipid-related metabolites and metabolites enriched in sphingolipid metabolic pathways. (J) Top 10 significantly enriched KEGG pathways based on differential metabolites. (K) GSEA of the sphingolipid signaling pathway. (L) ELISA measurement of S1P levels in serum, striatum, and prefrontal cortex.

Behavioral experiments were performed using $n = 10$ mice per group. Metabolomic profiling and ELISA analyses were performed using independent cohorts ($n = 8$ mice per group for ELISA). Data are presented as mean ± SEM. Statistical comparisons were performed using unpaired two-tailed t tests unless otherwise indicated. Differential metabolites were identified using an adjusted q value < 0.05 and $|\log_2 FC| > 1$. Statistical significance is indicated as $^{*}p < 0.05$, $^{**}p < 0.01$, $^{***}p < 0.001$, and $^{****}p < 0.0001$.

.

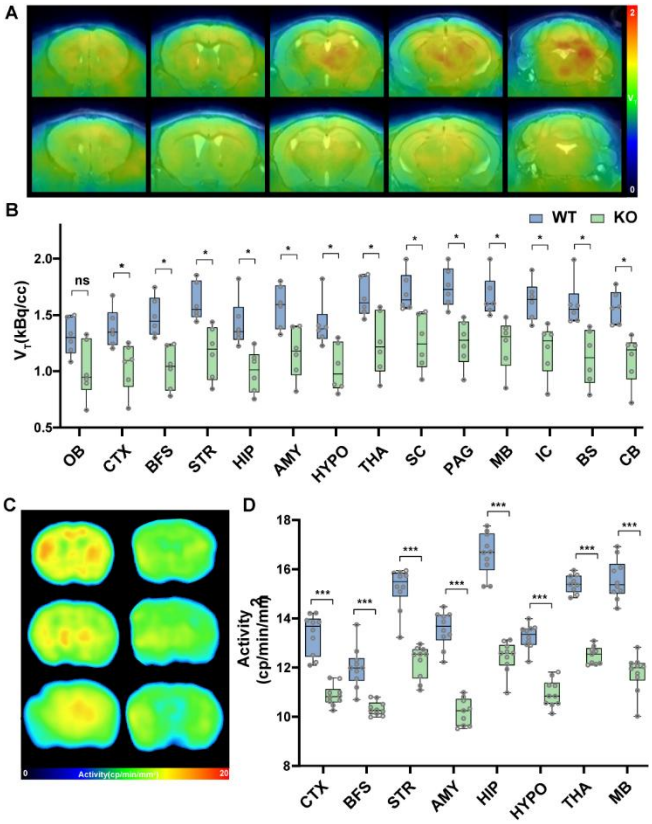


Figure 2. Brain-wide mapping of S1PR1 availability using [18F]TZ4877 PET imaging.

(A) Representative coregistered [^{18}F]TZ4877 PET-MRI images showing regional distributions of S1PR1 availability in WT and *Sapap3* KO mice (n = 6 per group). (B) Quantification of [^{18}F]TZ4877 PET-derived V_T values across multiple brain regions. (C) Representative autoradiography images showing the distribution of [^{18}F]TZ4877 binding in WT and *Sapap3* KO brains. (D) Quantification of autoradiographic [^{18}F]TZ4877 binding density across brain regions. Data are presented as mean ± SEM. Statistical comparisons between WT and *Sapap3* KO mice were performed using unpaired two-tailed t tests, with FDR correction applied for multiple regional comparisons. Statistical significance was defined as *$q < 0.05$.

Abbreviations: OB, olfactory bulb; CTX, cortex; BFS, basal forebrain septum; STR, striatum; THA, thalamus; HYP, hypothalamus; AMY, amygdala; HIP, hippocampus; SC, superior colliculus; IC, inferior colliculus; MB, midbrain; BS, brainstem; PAG, periaqueductal gray; CB, cerebellum.

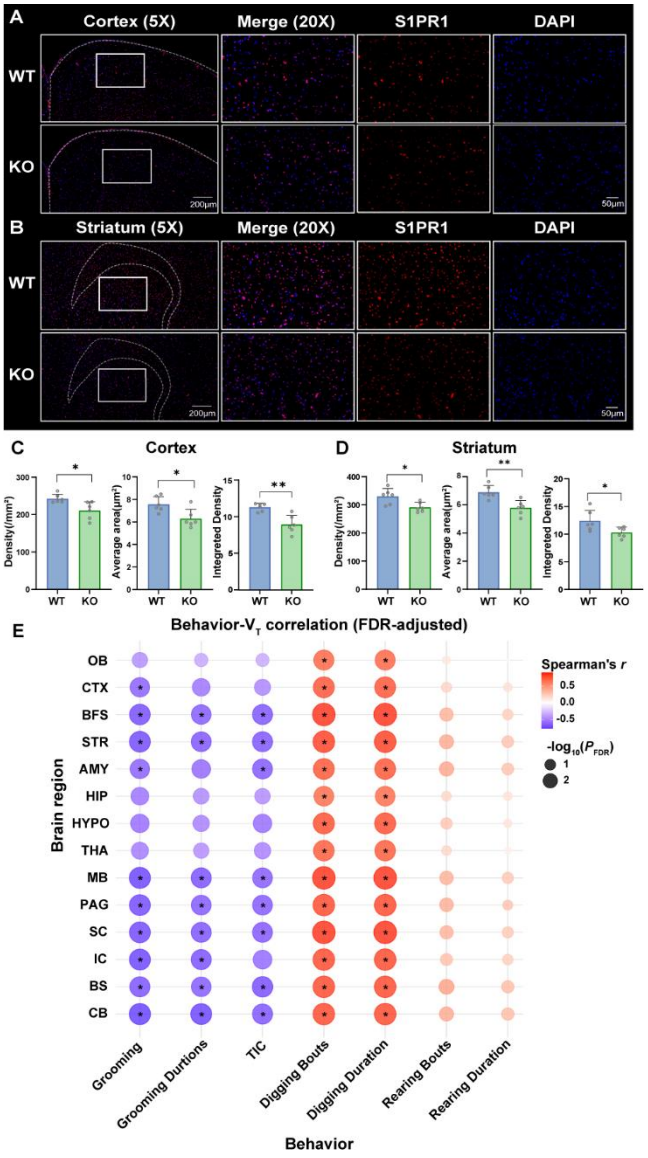


Figure 3. Immunofluorescence validation of S1PR1 alterations and behavioral associations.

(A–B) Representative immunofluorescence images showing S1PR1 immunoreactivity in the cortex (A) and striatum (B) of WT and *Sapap3* KO mice. Scale bars, 200 μm (low magnification) and 50 μm (high magnification). (C–D) Quantification of S1PR1 puncta density, puncta area, and integrated fluorescence intensity in the cortex (C) and striatum (D). (E) Spearman correlation analysis between regional S1PR1 V_T values and compulsive-like behavioral measures. Bubble size represents statistical significance ($-\log_{10}(P_{FDR})$), and color indicates correlation coefficients. Data are presented as mean ± SEM. Group comparisons were performed using unpaired two-tailed t tests. Behavioral associations were assessed using Spearman rank correlation analysis. Multiple comparisons were controlled using FDR correction. Statistical significance is indicated as $*p < 0.05$ and $**p < 0.01$. Abbreviations are the same as in Figure 2.

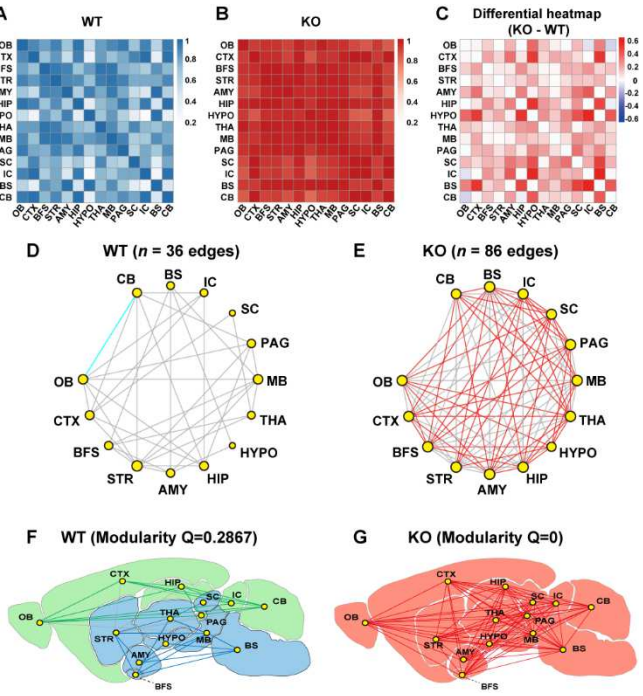


Figure 4. Whole-brain mapping of S1PR1 molecular covariance architecture.

(A–B) Whole-brain S1PR1 molecular covariance matrices derived from regional [^{18}F]TZ4877 PET V_T values in WT (A) and *Sapap3* KO (B) mice. Each matrix represents pairwise correlations in regional S1PR1 availability across 14 brain regions. (C) Differential covariance matrix showing genotype-associated changes in regional S1PR1 molecular covariance (S*apap3* KO − WT). (D–E) Graph-based visualization of WT (D) and *Sapap3* KO (E) S1PR1 molecular covariance architectures. (F–G) Spatial representation of S1PR1 molecular covariance architectures and modular organization in WT (F) and *Sapap3* KO (G) mice. Network modularity was quantified using community detection analysis applied to the S1PR1 molecular covariance matrices.

Abbreviations are the same as in Figure 2.

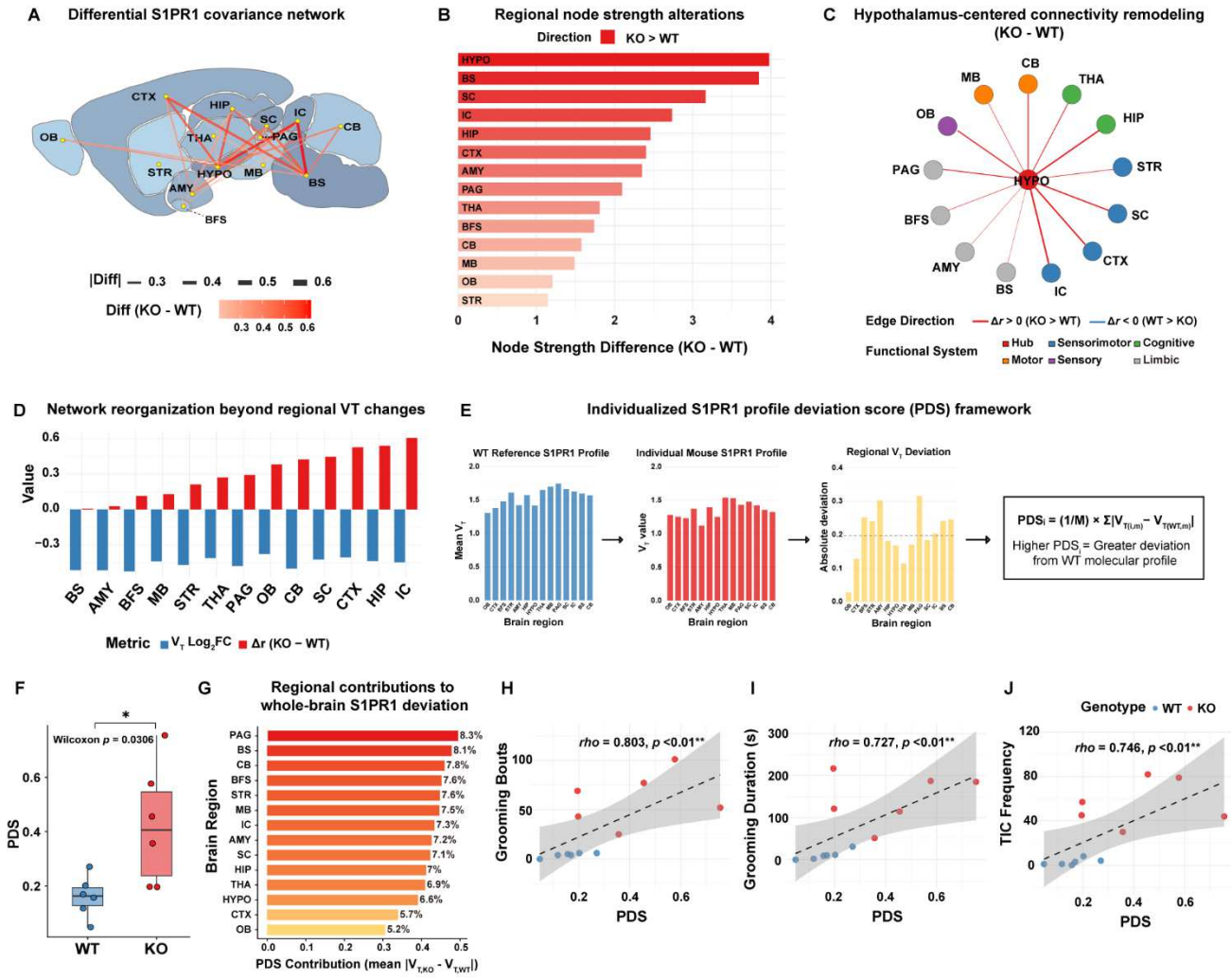


Figure 5. Hypothalamic-centered S1PR1 molecular covariance alterations and individualized molecular deviation profiling.

(A) Differential weighted S1PR1 molecular covariance network illustrating genotype-associated changes in interregional covariance after thresholding (|Diff| > 0.2). Edge width represents the magnitude of covariance alteration, and edge color indicates the direction of covariance change. (B) Ranking of regional node strength changes ($\Delta S = S_{KO} - S_{WT}$) across 14 brain regions. (C) Hypothalamus-centered S1PR1 molecular covariance architecture. (D) Association between regional changes in S1PR1 V_T and hypothalamus-centered covariance alterations. Statistical analyses and network construction procedures are described in the Methods. (E) Schematic illustration of the individualized S1PR1 PDS calculation. Each mouse's regional S1PR1 V_T profile was compared with the WT reference profile, and mean absolute deviation across brain regions was calculated to generate the individualized S1PR1 PDS. (F) Comparison of whole-brain S1PR1 PDS between WT and

Sapap3 KO mice. (G) Regional contributions to whole-brain S1PR1 profile deviation scores. (H–J) Correlations between individual PDS values and compulsive-like behavioral measures, including grooming bout frequency (H), grooming duration (I), and tic frequency (J). Data are presented as individual values. Group comparisons were performed using the Wilcoxon rank-sum test, and associations between PDS values and behavioral measures were assessed using Spearman rank correlation analysis. Statistical significance is indicated as $*p < 0.05$, $**p < 0.01$. Abbreviations are the same as in Figure 2.

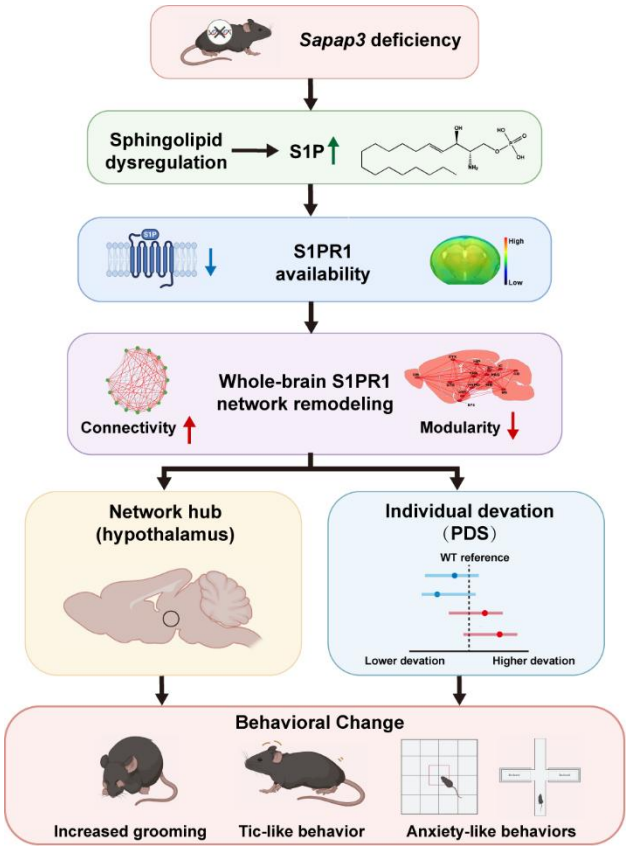


Figure 6. Integrated framework summarizing S1P–S1PR1 alterations, brain-wide molecular organization, and compulsive-like behaviors.

Conceptual framework summarizing observed associations among sphingolipid metabolism, S1PR1 availability, molecular covariance organization, individualized molecular deviation, and compulsive-like behavioral phenotypes. The framework integrates increased S1P abundance, reduced regional S1PR1 availability estimated by [^{18}F]TZ4877 PET-derived V_T values, and whole-brain S1PR1 molecular covariance alterations. These receptor-level alterations are associated with changes in brain-wide molecular organization, including altered interregional covariance and modular architecture. Network-level analysis identifies the hypothalamus as a prominent node within the altered S1PR1 molecular covariance architecture, whereas individualized S1PR1 PDS captures inter-individual molecular deviation associated with compulsive-like behavioral phenotypes. Together, these multiscale associations summarize a receptor-level molecular framework connecting S1P–S1PR1 biology, brain-wide molecular organization, and behavioral heterogeneity.

Supplementary Files

This is a list of supplementary files associated with this preprint. Click to download.

- Supplementary.docx